DALTON
FULL PAPER

Synthesis and characterisation of thiolato Schiff base nickel(II) complexes. X-Ray structures of $Ni(\eta^5\text{-}C_5H_5)(PPh_3)(SC_6H_4N{=}CHC_6H_4Br\text{-}4')$ and $Ni(\eta^5\text{-}C_5H_5)(PBu_3)(SC_6H_4N{=}CHC_6H_4CH_3\text{-}4')$ ‡

Funzani A. Nevondo, Andrew M. Crouch † and James Darkwa *

Department of Chemistry, University of the Western Cape, Private Bag X17, Bellville 7535, South Africa. E-mail: jdarkwa@uwc.ac.za

Received 27th August 1999, Accepted 4th November 1999

A series of complexes of formula $Ni(\eta^5\text{-}C_5H_5)(PR_3)(SC_6H_4N{=}CHC_6H_4X\text{-}4')$ (R = Ph, Bu; X = F, Cl, Br, CH_3, OH, H) has been isolated from the reactions of $Ni(\eta^5\text{-}C_5H_5)(PPh_3)Cl$ or the bromo derivative, the thiol Schiff base ligands, $4\text{-}HSC_6H_4N{=}CHC_6H_4X\text{-}4'$, and triethylamine. Preliminary thermal analysis data indicate that the PBu_3 complexes could exhibit liquid crystalline behaviour. Electrochemistry of the PPh_3 compounds gave irreversible redox couples, in contrast to the quasi-reversibility of the PBu_3 compounds.

Introduction

Early investigations of Schiff bases that contain imine nitrogen and anionic sulfur ligands centred on their use as biological models.[1] These were usually metal complexes of the ligands, formed *in situ* from the condensation of 2-mercaptoaniline and a carbonyl compound in the presence of a metal ion.[2] The ligands bind in a bidentate fashion through the nitrogen and the sulfur atoms. Without this *in situ* approach, the condensation products of the 2-mercaptoaniline and the carbonyl compound result in an undesirable cyclization to form heterocyclic compounds;[3] though the cyclized products exist in equilibrium with a small amount of a non-cyclized thiol compound.[4] Some of the recent work on Schiff base ligands has however concentrated on their potential use in materials science; specifically liquid crystals[5] and non-linear optical materials.[6] In such applications, it is anticipated that the presence of a metal in a complex that contains a Schiff base would modify the properties of the complex. In particular, Schiff base ligands that can bind two metal centers as bridging ligands and posses delocalised π-electrons could function as conducting materials.

Our interest in the synthesis and charaterization of nickel(II) thiolato complexes[7] has been extended to thiolato Schiff base ligands. We expect, in this approach, to use these Schiff base ligand complexes as building blocks for preparing compounds that could be used as liquid crystals and conducting materials. Schiff base complexes that behave as metallomesogens are of two types. The first type are complexes where the Schiff base is bound to a metal.[8] This includes a number of tetradentate nickel Schiff base compounds[9] (Chart 1). The second type are complexes where the Schiff base ligand is attached to a ligand bound to a metal *via* atoms other than the imine unit. These latter compounds are substituted ferrocenes, with one of the cyclopentadienyl ligands carrying the Schiff base[6,10] (Chart 1). Apart from nickel Schiff base metallomesogens, nickel thiolates[11,12] and dithiolene[13] compounds also show a range of liquid crystalline behaviour. The dinuclear complexes, $Ni_2(S_2CR)_4$ ($R = C_nH_{2n+1}$), exhibit monotropic lamellar mesophases when $n = 4$ or 8.[12]

In this project we have combined the potential of Schiff base ligands to form metallomesogens with that of the thiolate ligands to synthesize nickel thiolato Schiff base complexes. The result is the synthesis of a new class of nickel thiolato Schiff base compounds with potential mesogenic behaviour.

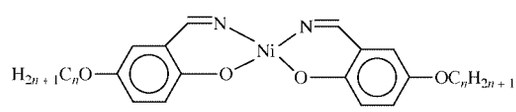

($n = 5$ or 12)

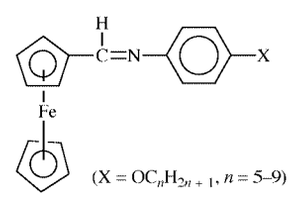

($X = OC_nH_{2n+1}$, $n = 5$–9)

A

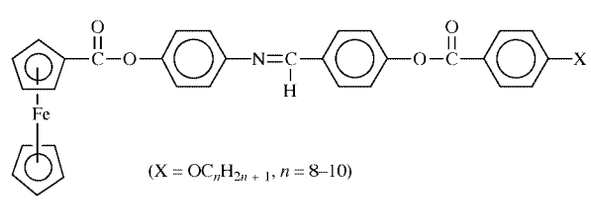

($X = OC_nH_{2n+1}$, $n = 8$–10)

B

Chart 1

Experimental

Materials and instrumentation

All solvents were dried by procedures described as previously reported.[7c] All the commercially available chemicals were used as received. The nickel starting materials, $Ni(\eta^5\text{-}C_5H_5)(PPh_3)Cl$,[14] $Ni(\eta^5\text{-}C_5H_5)(PPh_3)Br$[14] and $Ni(\eta^5\text{-}C_5H_5)(PBu_3)Cl$,[15] were prepared by the literature procedures. Infrared spectra were recorded on a Perkin-Elmer Paragon 1000PC FT spectrometer as Nujol mulls. The ^1H, ^{13}C and ^{31}P NMR spectra were recorded on a Varian Gemini 2000 and referenced to residual $CHCl_3$ for ^1H (δ 7.26), ^{13}C (δ 77.0) and to PPh_3 (δ −5.00) for ^{31}P. Mass spectra of ligands were recorded on a Finnigan MAT GCQ GC/MS. The mass spectra of the metal complexes were

† *Present address*: Department of Chemistry, University of Stellenbosch, Private Bag X1, Matieland 7602, South Africa.
‡ *Supplementary data available*: rotatable 3-D crystal structure diagram in CHIME format. See http://www.rsc.org/suppdata/dt/a9/a906949f/

recorded on a JEOL JMS-HX100 EBE in the FAB mode, using nitrobenzyl alcohol as the matrix as described previously.[16] Thermal analyses were performed on a Perkin-Elmer TGA-7 and a Perkin-Elmer DSC-7 at a heating rate of 10 °C min^{-1} under nitrogen. Elemental analyses were performed in-house with a CARLO ERBA NA analyzer.

Electrochemical measurements

Cyclic voltammetric measurements were performed on a BAS-C50W electrochemical analyzer at room temperature, using sample concentrations of 10^{-3} M. Tetra-*n*-butylammonium tetrafluoroborate was used as supporting electrolyte. A three-electrode configuration, consisting of a platinum working electrode a platinum wire as auxiliary electrode and Ag/AgCl reference electrode was employed. The ferrocene/ferrocenium couple (+0.46 V *vs.* Ag/AgCl in CH_2Cl_2) was used as an internal standard. High purity and dry dichloromethane was used as the solvent and experiments were performed under dry nitrogen.

Syntheses

Schiff base ligands. The thioimines, 4-$HSC_6H_4N{=}CHC_6H_4$-X-4′ (X = F **1a**, Cl **2a**, Br **3a**, CH_3 **4a**, OH **5a**, H **6a**), were prepared by the following general procedure. To a solution of 4-aminothiophenol in ethanol (50 mL) was added the appropriate *para*-substituted benzaldehyde in a 1 : 1 mole ratio and the solution stirred at room temperature for 6–24 h. The initial yellow solutions gave precipitates within 30 min, except for the hydroxy derivative, **5a**. The precipitates were isolated by suction filtration and recrystallized from CH_2Cl_2–hexane. In isolating **5a**, the clear solution was first evaporated to dryness and the residue recrystallized from CH_2Cl_2–hexane. The yields were generally moderate to high, 60–86%.

*Complex **1a**.* Yield: 63%. Anal. Calc. for $C_{13}H_{10}FNS$: C, 67.51; H, 4.36; N, 6.06. Found: C, 66.96; H, 4,41; N, 5.86%. ^{1}H NMR ($CDCl_3$): δ 8.41 (s, 1H, N=CH); 7.33 (m, 6H, $SC_6H_4N{=}CHC_6H_4F$-4′); 6.59 (d, 2H, J_{HH} = 8.80 Hz, $SC_6H_4N{=}CHC_6H_4$-F-4′); 3.49 (s, 1H, SH). IR (Nujol mull, cm^{-1}): ν(C=N) 1591. MS (EI): m/z = 231 (M^+, 100%).

*Complex **2a**.* Yield: 71%. Anal. Calc. for $C_{13}H_{10}ClNS$: C, 63.03; H, 4.04; N, 5.65. Found: C, 63.19; H, 3.98; N, 5.63%. ^{1}H NMR ($CDCl_3$): δ 8.41 (s, 1H, N=CH); 7.42 (m, 6H, $SC_6H_4N{=}CHC_6H_4Cl$-4′); 6.59 (d, J_{HH} = 8.80 Hz, 2H, $SC_6H_4N{=}CHC_6H_4Cl$-4′); 3.49 (s, 1H, SH). IR (Nujol mull, cm^{-1}): ν(C=N) 1591. MS (EI): m/z = 247 (M^+, 100%).

*Complex **3a**.* Yield: 74%. Anal. Calc. for $C_{13}H_{10}BrNS$: C, 53.44; H, 3.42; N, 4.79. Found: C, 53.23; H, 3.49; N, 4.68%. ^{1}H NMR ($CDCl_3$): δ 8.39 (s, 1H, N=CH); 7.32 (m, 8H, $SC_6H_4N{=}CHC_6H_4Br$-4′); 3.49 (s, 1H, SH). IR (Nujol mull, cm^{-1}): ν(C=N) 1590. MS (EI): m/z = 293 (M^+, 100%).

*Complex **4a**.* Yield: 86%. Anal. Calc. for $C_{14}H_{13}NS$: C, 74.00; H, 5.72; N, 6.16. Found: C, 74.02; H, 6.12; N, 5.90%. ^{1}H NMR ($CDCl_3$): δ 8.39 (s, 1H, N=CH); 7.78 (d, J_{HH} = 8.00 Hz, 2H, $SC_6H_4N{=}CHC_6H_4CH_3$-4′); 7.25 (m, 4H, $SC_6H_4N{=}CHC_6H_4$-CH_3-4′); 6.58 (d, J_{HH} = 8.80 Hz, 2H, $SC_6H_4N{=}CHC_6H_4CH_3$-4′); 3.47 (s, 1H, SH); 2.09 (s, 3H, $SC_6H_4N{=}CHC_6H_4CH_3$-4′). IR (Nujol mull, cm^{-1}): ν(C=N) 1602. MS (EI): m/z = 227 (M^+, 100%).

*Complex **5a**.* Yield: 70%. Anal. Calc. for $C_{13}H_{11}NOS$: C, 68.12; H, 4.80; N, 6.11. Found: C, 66.91; H, 5.15; N, 6.14%. ^{1}H NMR (d^6-DMSO): δ 8.40 (s, 1H, N=CH); 7.50 (m, 8H, $SC_6H_4N{=}CHC_6H_4OH$-4′); 3.50 (s, 1H, SH). IR (Nujol mull, cm^{-1}): ν(C=N) 1600. MS (EI): m/z = 229 (M^+, 100%).

*Complex **6a**.* Yield: 75%. Anal. Calc. for $C_{13}H_{11}NS$: C, 73.23; H, 5.16; N, 6.57. Found: C, 73.13; H, 5.90; N, 6.57%. ^{1}H NMR ($CDCl_3$): δ 8.44 (s, 1H, N=CH); 7.88 (m, 2H, $SC_6H_4N{=}CHC_6H_5$); 7.48 (m, 3H, $SC_6H_4N{=}CHC_6H_5$); 7.32 (d, J_{HH} = 8.40 Hz, 2H, $SC_6H_4N{=}CHC_6H_5$); 7.12 (d, J_{HH} = 8.60 Hz, $SC_6H_4N{=}CHC_6H_5$); 3.49 (s, 1H, SH). IR (Nujol mull, cm^{-1}): ν(C=N) 1597. MS (EI): m/z = 213 (M^+, 100%).

Reaction of Ni(η^5-C_5H_5)(PPh_3)Br with 4-$HSC_6H_4N{=}CHC_6H_4$-X-4′: formation of Ni(η^5-C_5H_5)(PPh_3)($SC_6H_4N{=}CHC_6H_4$X-4′) (X = F 1b, Cl 2b, Br 3b, CH_3 4b, OH 5b, H 6b)

In a typical reaction a mixture of Ni(η^5-C_5H_5)(PPh_3)Br (0.63 g, 1.29 mmol) and **1a** (0.30 g, 1.28 mmol) was degassed. Addition of degassed toluene (75 mL), followed by Et_3N (0.5 mL) immediately changed the solution from purple to brownish-green. After stirring for 4 h the mixture was filtered to remove solid Et_3NHBr by-product. The filtrate was concentrated to about 20 mL; an equal volume of hexane was added and the solution cooled at −15 °C to precipitate the product. Recrystallization from CH_2Cl_2–hexane gave dark green crystalline **1b**. Yield 62%. Anal. Calc. for $C_{36}H_{29}FNPSNi$: C, 70.15; H, 4.74; N, 2.27. Found: C, 70.08; H, 4.61; N, 2.35%. ^{1}H NMR ($CDCl_3$): δ 8.43 (s, 1H, N=CH); 7.86 (dd, J_{HH} = 8.40 Hz, J_{HF} = 5.80 Hz, 2H, $SC_6H_4N{=}CHC_6H_4F$-4′), 7.69 (m, 6H, PPh_3); 7.39 (m, 11H, PPh_3, $SC_6H_4N{=}CHC_6H_4F$-4′); 7.13 (t, J_{HH}/J_{HF} = 8.20 Hz, 2H, $SC_6H_4N{=}CHC_6H_4F$-4′); 6.87 (d, J_{HH} = 8.40 Hz, 2H, $SC_6H_4N{=}CHC_6H_4F$-4′); 5.14 (s, 5H, C_5H_5). $^{13}C\{^1H\}$ NMR ($CDCl_3$): δ 154.1 (s, N=CH); 144.2 (s); 132.2 (s); 131.7 (d, J_{CP} = 42.0 Hz); 131.4 (s); 130.5 (s); 128.6 (s); 128.4 (s); 128.2 (d, J_{CP} = 10.6 Hz); 126.4 (d, J_{CP} = 41.0 Hz); 118.2 (s); 114.1 (s); 113.7 (s); 92.1 (s). $^{31}P\{^1H\}$ NMR ($CDCl_3$): δ 35.38 (s, PPh_3). IR (Nujol mull, cm^{-1}): ν(C=N) 1597. MS (FAB): m/z = 615 (M^+, 8%).

All the PPh_3 complexes were prepared and worked up in a similar manner as described above. Their analytical data were as reported below.

Complex 2b. Yield 66%. Anal. Calc. for $C_{36}H_{29}ClNPSNi$: C, 68.33; H, 6.20; N, 2.21. Found: C, 67.41; H, 4.48; N, 2.21%. ^{1}H NMR ($CDCl_3$): δ 8.43 (s, 1H, N=CH); 7.81 (d, J_{HH} = 8.40 Hz, 2H, $SC_6H_4N{=}CHC_6H_4Cl$-4′), 7.69 (m, 6H, PPh_3); 7.38 (m, 13H, PPh_3, $SC_6H_4N{=}CHC_6H_4Cl$-4′); 6.87 (d, J_{HH} = 8.40 Hz, 2H, $SC_6H_4N{=}CHC_6H_4Cl$-4′); 5.14 (s, 5H, C_5H_5). $^{13}C\{^1H\}$ NMR ($CDCl_3$): δ 156.6 (s, N=CH); 146.6 (s); 145.2 (s); 137.4 (s); 135.9 (s); 134.8 (s); 134.4 (d, J_{CP} = 42.0 Hz); 134.0 (s); 133.1 (s); 130.9 (d, J_{CP} = 9.2 Hz); 129.7 (s); 129.0 (d, J_{CP} = 41.0 Hz); 120.9 (s); 94.7 (s). $^{31}P\{^1H\}$ NMR ($CDCl_3$): δ 35.37 (s, PPh_3). IR (Nujol mull, cm^{-1}): ν(C=N) 1590. MS (FAB): m/z = 631 (M^+, 3%).

Complex 3b. Yield 70%. Anal. Calc. for $C_{36}H_{29}BrNPSNi$: C, 63.79; H, 4.31; N, 2.06. Found: C, 64.01; H, 4.27; N, 1.99%. ^{1}H NMR ($CDCl_3$): δ 8.41 (s, 1H, N=CH); 7.71 (m, 8H, PPh_3, $SC_6H_4N{=}CHC_6H_4Br$-4′); 7.58 (d, J_{HH} = 8.40 Hz, 2H, $SC_6H_4N{=}CHC_6H_4Br$-4′); 7.38 (m, 11H, PPh_3, $SC_6H_4N{=}CHC_6H_4Cl$-4′); 6.87 (d, J_{HH} = 8.40 Hz, 2H, $SC_6H_4N{=}CHC_6H_4Br$-4′); 5.14 (s, 5H, C_5H_5). $^{13}C\{^1H\}$ NMR ($CDCl_3$): δ 156.6 (s, N=CH); 146.5 (s); 136.3 (s); 134.8 (s); 134.4 (d, J_{CP} = 42.00 Hz); 134.0 (s); 133.1 (s); 132.7 (s); 130.9 (d, J_{CP} = 9.00 Hz); 130.6 (s); 129.0 (d, J_{CP} = 40.80 Hz); 125.9 (s); 120.9 (s); 94.7 (s). $^{31}P\{^1H\}$ NMR ($CDCl_3$): δ 35.37 (s, PPh_3). IR (Nujol mull, cm^{-1}): ν(C=N) 1587.

Complex 4b. Yield 67%. Anal. Calc. for $C_{37}H_{32}NPSNi$: C, 72.65; H, 5.27; N, 2.28. Found: C, 73.16; H, 5.39; N, 2.25%. ^{1}H NMR ($CDCl_3$): δ 8.43 (s, 1H, N=CH); 7.70 (m, 8H, PPh_3, $SC_6H_4N{=}CHC_6H_4CH_3$-4′); 7.38 (m, 11H, PPh_3, $SC_6H_4N{=}CHC_6H_4CH_3$-4′); 7.25 (d, J_{HH} = 8.40 Hz, 2H, $SC_6H_4N{=}CHC_6H_4CH_3$-4′); 6.87 (d, J_{HH} = 8.40 Hz, 2H, $SC_6H_4N{=}CHC_6H_4CH_3$-4′); 5.14 (s, 5H, C_5H_5); 2.39 (s, 3H, $SC_6H_4N{=}CHC_6H_4CH_3$-4′). $^{13}C\{^1H\}$ NMR ($CDCl_3$): δ 157.7 (s, N=CH); 143.4 (s); 134.2 (s); 133.7 (d, J_{CP} = 42.40 Hz); 132.4 (s); 130.2 (d, J_{CP} = 10.60 Hz); 129.5 (s); 128.5 (s); 128.3 (d, J_{CP} = 40.80 Hz); 120.2 (s); 94.0 (s); 21.5 (s). $^{31}P\{^1H\}$ NMR ($CDCl_3$): δ 35.41 (s, PPh_3). IR (Nujol mull, cm^{-1}): ν(C=N) 1602. MS (FAB): m/z = 611 (M^+, 15%).

Complex 5b. Yield 67%. Anal. Calc. for $C_{36}H_{30}NOPSNi$: C,

70.38; H, 4.92; N, 2.28. Found: C, 68.71; H, 4.68; N, 2.41%. ^{1}H NMR ($CDCl_3$): δ 8.37 (s, 1H, N=CH); 7.69 (m, 8H, PPh_3, SC_6H_4N=CHC_6H_4OH-4′); 7.35 (m, 11H, PPh_3, SC_6H_4N=CHC_6H_4OH-4′); 7.25 (d, J_{HH} = 8.40 Hz, 2H, SC_6H_4N=CHC_6H_4OH-4′); 6.86 (dd, J_{HH} = 8.60 Hz, J_{HH} = 4.00 Hz, 4H, SC_6H_4N=CHC_6H_4OH-4′); 5.13 (s, 5H, C_5H_5). $^{13}C\{^1H\}$ NMR ($CDCl_3$): δ 154.2 (s, N=CH); 136.1 (s); 136.0 (s); 132.3 (s); 131.7 (d, J_{CP} = 42.40 Hz); 130.0 (s); 128.6 (s); 128.2 (s); 126.4 (d, J_{CP} = 40.80 Hz); 118.1 (s); 113.8 (s); 92.1 (s). $^{31}P\{^1H\}$ NMR ($CDCl_3$): δ 35.43 (s, PPh_3). IR (Nujol mull, cm^{-1}): ν(C=N) 1604. MS (FAB): m/z = 613 (M^+, 50%).

Complex 6b. Yield: 73%. Anal. Calc. for $C_{36}H_{30}NPSNi$: C, 72.26; H, 5.05; N, 2.34. Found: C, 72.10; H, 5.10; N, 2.35%. ^{1}H NMR ($CDCl_3$): δ 8.47 (s, 1H, N=CH); 7.83 (m, 2H, SC_6H_4N=CHC_6H_5); 7.69 (m, 6H, PPh_3); 7.39 (m, 14H, PPh_3, SC_6H_4N=CHC_6H_5); 6.83 (d, J_{HH} = 8.40 Hz, 2H, SC_6H_4N=CHC_6H_5); 5.14 (s, 5H, C_5H_5). $^{13}C\{^1H\}$ NMR ($CDCl_3$): δ 157.6 (s, N=CH); 146.4 (s); 134.2 (s); 133.7 (d, J_{CP} = 42.66 Hz); 133.4 (s); 132.5 (s); 132.2 (s); 130.2 (d, J_{CP} = 10.60 Hz); 128.6 (d, J_{CP} = 36.40 Hz); 128.3 (d, J_{CP} = 40.00 Hz); 120 (s); 92.1 (s). $^{31}P\{^1H\}$ NMR ($CDCl_3$): δ 35.36 (s, PPh_3). IR (Nujol mull, cm^{-1}): ν(C=N) 1581.

Reaction of Ni(η^5-C_5H_5)(PBu_3)Cl with 4-HSC_6H_4N=CHC_6H_4-X-4′: formation of Ni(η^5-C_5H_5)(PBu_3)(SC_6H_4N=CHC_6H_4X-4′) (X = F 1c, Cl 2c, Br 3c, CH_3 4c, H 6c)

To a solution of 4-HSC_6H_4N=CHC_6H_4F-4′ **1a** (0.35 g, 1.38 mmol) in toluene (25 mL) was added a solution of Ni(η^5-C_5H_5)(PBu_3)Cl (0.53 g, 1.38 mmol) in toluene (25 mL) *via* a pressure equalizing dropping funnel. Addition of excess Et_3N (1.0 mL) gradually changed the purple solution to brown. After stirring the reaction mixture for 18 h, it was filtered to remove Et_3NHCl as a by-product. The solvent was removed under reduced pressure and the residue recrystallized from CH_2Cl_2–hexane and isolated as dark brown crystalline **1c**. Yield 69%. Anal. Calc. for $C_{30}H_{44}FNPSNi$: C, 64.79; H, 7.37; N, 2.52. Found: C, 64.02; H, 7.81; N, 2.57%. ^{1}H NMR ($CDCl_3$): δ 8.44 (s, 1H, N=CH); 7.88 (dd, J_{HH} = 8.80 Hz, J_{HF} = 5.60 Hz, 2H, SC_6H_4N=CHC_6H_4F-4′); 7.63 (d, J_{HH} = 8.20 Hz, 2H, SC_6H_4N=CHC_6H_4F-4′); 7.13 (t, J_{HF} = 8.60, 2H, SC_6H_4N=CHC_6H_4F-4′); 6.95 (d, J_{HH} = 8.40 Hz, 2H, SC_6H_4N=CHC_6H_4F-4′); 5.27 (s, 5H, C_5H_5); 1.43 (m, 18H, PBu_3); 0.92 (t, J_{HH} = 7.00 Hz, 9H, PBu_3). $^{13}C\{^1H\}$ NMR ($CDCl_3$): δ 155.9 (s, N=CH), 145.9 (s); 144.7 (s); 133.7 (s); 133.0 (s); 130.4 (d, J_{CF} = 86.60 Hz); 120.0 (s); 115.8 (d, J_{CF} = 86.60 Hz); 91.8 (s); 26.3 (s); 24.5 (d, J_{CP} = 112.00 Hz); 21.1 (d, J_{CP} = 53.20 Hz); 13.7 (s). $^{31}P\{^1H\}$ NMR ($CDCl_3$): δ 22.41 (s, PBu_3). IR (Nujol mull, cm^{-1}): ν(C=N) 1601.

Complex 2c. Yield 66%. Anal. Calc. for $C_{30}H_{44}ClNPSNi$: C, 62.94; H, 7.16; N, 2.45. Found: C, 62.63; H, 7.51; N, 2.38%. ^{1}H NMR ($CDCl_3$): δ 8.44 (s, 1H, N=CH); 7.81 (d, J_{HH} = 8.60 Hz, 2H, SC_6H_4N=CHC_6H_4Cl-4′); 7.63 (d, J_{HH} = 8.40 Hz, 2H, SC_6H_4N=CHC_6H_4Cl-4′); 7.41 (d, J_{HH} = 8.60 Hz, 2H, SC_6H_4N=CHC_6H_4Cl-4′); 6.96 (d, J_{HH} = 8.40 Hz, 2H, SC_6H_4N=CHC_6H_4Cl-4′); 5.27 (s, 5H, C_5H_5); 1.48 (m, 18H, PBu_3); 0.92 (t, J_{HH} = 7.00 Hz, 9H, PBu_3). $^{13}C\{^1H\}$ NMR ($CDCl_3$): δ 155.7 (s, N=CH); 145.2 (s); 136.7 (s); 135.3 (s); 133.7 (s); 129.0 (s); 128.9 (s); 120.3 (s); 91.9 (s); 26.3 (d, J_{CP} = 4.60 Hz); 24.2 (d, J_{CP} = 53.20 Hz); 22.5 (d, J_{CP} = 110.60 Hz); 13.6 (s). $^{31}P\{^1H\}$ NMR ($CDCl_3$): δ 22.43 (s, PBu_3). IR (Nujol mull, cm^{-1}): ν(C=N) 1589.

Complex 3c. Yield 64%. Anal. Calc. for $C_{30}H_{44}BrNPSNi$: C, 58.40; H, 6.65; N, 2.27. Found: C, 58.80; H, 6.80; N, 2.63%. ^{1}H NMR ($CDCl_3$): δ 8.44 (s, 1H, N=CH); 7.81 (d, J_{HH} = 8.60 Hz, 2H, SC_6H_4N=CHC_6H_4Br-4′); 7.62 (d, J_{HH} = 8.60 Hz, 2H, SC_6H_4N=CHC_6H_4Br-4′); 7.42 (d, J_{HH} = 8.40 Hz, 2H, SC_6H_4N=CHC_6H_4Br-4′); 6.96 (d, J_{HH} = 8.40 Hz, 2H, SC_6H_4N=CHC_6H_4Br-4′); 5.27 (s, 5H, C_5H_5); 1.49 (m, 18H, PBu_3); 0.93 (t, J_{HH} = 7.00 Hz, 9H, PBu_3). $^{13}C\{^1H\}$ NMR ($CDCl_3$): δ 153.8 (s, N=CH); 143.7 (s); 143.2 (s); 134.7 (s); 133.3 (s); 131.7 (s); 127.7 (s); 127.3 (s); 118.3 (s); 89.9 (s); 24.3 (s); 22.5 (d, J_{CP} = 110.60 Hz); 22.2 (d, J_{CP} = 53.20 Hz); 11.7 (s). $^{31}P\{^1H\}$ NMR ($CDCl_3$): δ 22.45 (s, PBu_3). IR (Nujol mull, cm^{-1}): ν(C=N) 1592.

Table 1 Crystal data for **3b** and **4c**

	3b	**4c**
Formula	$C_{36}H_{29}BrNPSNi$	$C_{31}H_{47}NPSNi$
FW	677.25	552.41
T/K	296(2)	293(2)
λ/Å	0.71073	0.71070
Crystal system	Monoclinic	Triclinic
Space group	$P2_1/n$	$P\bar{1}$
a/Å	10.833(5)	10.809(1)
b/Å	14.848(5)	10.916(1)
c/Å	19.742(9)	14.430(1)
α/°		80.813(2)
β/°	102.899(10)	73.796(2)
γ/°		68.446(2)
V/Å^3	3095.0(2)	1517.5(1)
Z	4	4
D_{calc}/Mg m^{-3}	1.4531	1.209
μ/mm^{-1}	2.063	0.780
F(000)	1384	592
Crystal size/mm	0.80 × 0.54 × 0.06	0.21 × 0.35 × 0.28
No. of reflections collected/unique	17906/6929	13355/6780
R(int.)	0.045	0.044
Data/restraints/parameters	6929/0/486	8801/0/305
Final R indices [$I > 2\sigma(I)$]	R_1 = 0.0525, wR_2 = 0.1363	R_1 = 0.0651, wR_2 = 0.1605
R indices (all data)	R_1 = 0.0847, wR_2 = 0.1568	R_1 = 0.0794, wR_2 = 0.1704
Largest difference peak and hole/e Å^{-3}	0.584, −0.462	3.0, −3.1

Complex 4c. Yield 73%. Anal. Calc. for $C_{31}H_{47}NPSNi$: C, 67.03; H, 8.53; N, 2.53. Found: C, 67.23; H, 8.60; N, 2.64%. ^{1}H NMR ($CDCl_3$): δ 8.43 (s, 1H, N=CH); 7.76 (d, J_{HH} = 8.40 Hz, 2H, SC_6H_4N=$CHC_6H_4CH_3$-4′); 7.61 (d, J_{HH} = 8.60 Hz, 2H, SC_6H_4N=$CHC_6H_4CH_3$-4′); 7.25 (d, J_{HH} = 8.00 Hz, 2H, SC_6H_4N=$CHC_6H_4CH_3$-4′); 6.95 (d, J_{HH} = 8.40 Hz, 2H, SC_6H_4N=$CHC_6H_4CH_3$-4′); 5.26 (s, 5H, C_5H_5); 2.40 (s, 3H, SC_6H_4N=$CHC_6H_4CH_3$-4′); 1.47 (m, 18H, PBu_3); 0.92 (t, J_{HH} = 7.00 Hz, 9H, PBu_3). $^{13}C\{^1H\}$ NMR ($CDCl_3$): δ 155.6 (s, N=CH); 144.5 (s); 142.0 (s); 139.3 (s); 132.2 (s); 131.7 (s); 127.5(s); 126.6 (s); 118.3 (s); 89.9 (s); 24.3 (s); 24.3 (s); 22.5 (d, J_{CP} = 28.22 Hz); 22.2 (d, J_{CP} = 13.38 Hz); 19.5 (s); 11.7 (s). $^{31}P\{^1H\}$ NMR ($CDCl_3$): δ 22.45 (s, PBu_3). IR (Nujol mull, cm^{-1}): ν(C=N) 1607.

Complex 6c. Yield 70%. Anal. Calc. for $C_{30}H_{45}NPSNi$: C, 66.93; H, 7.81; N, 2.60. Found: C, 66.80; H, 8.06; N, 2.52%. ^{1}H NMR ($CDCl_3$): δ 8.48 (s, 1H, N=CH); 7.86 (d, J_{HH} = 8.40 Hz, 2H, SC_6H_4N=CHC_6H_5); 7.62 (d, J_{HH} = 8.60 Hz, 2H, SC_6H_4N=CHC_6H_5); 7.45 (t, J_{HH} = 7.40 Hz, 3H, SC_6H_4N=CHC_6H_5); 6.96 (d, J_{HH} = 8.60 Hz, 2H, SC_6H_4N=CHC_6H_5); 5.27 (s, 5H, C_5H_5); 1.54 (m, 18H, PBu_3); 0.92 (t, J_{HH} = 7.20 Hz, 9H, PBu_3). $^{31}P\{^1H\}$ NMR ($CDCl_3$): δ 22.41 (s, PBu_3). IR (Nujol mull, cm^{-1}): ν(C=N) 1615.

Crystal structure determination of 3b

The structures of **3b** and **4c** were determined using a Siemens SMART and Enraf-Nonius Kappa diffractometers respectively, with graphite-monochromated Mo-Kα radiation (λ = 0.71073 Å). The crystal data, a summary of data collection and structure refinement are given in Table 1. The structures were solved by the Patterson method for primary atom sites and by difference map for atoms in secondary sites.[17] All non-hydrogen atoms were refined anisotropically and hydrogen atoms were

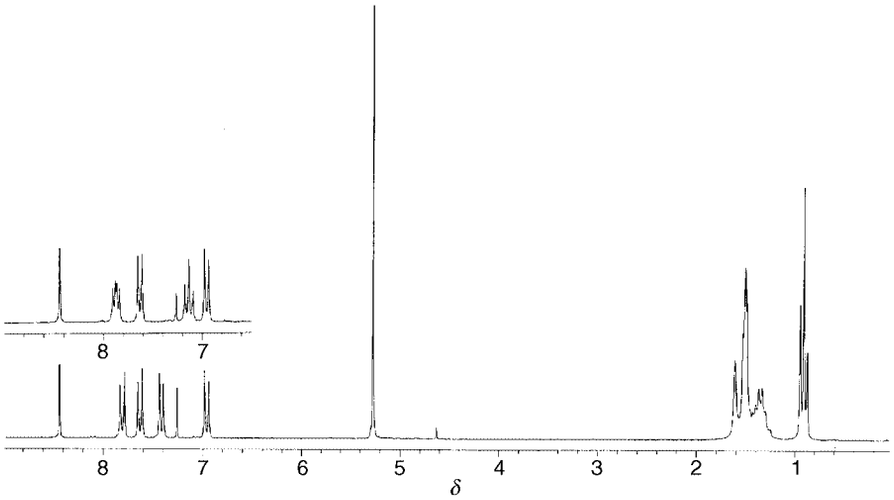

Fig. 1 ^{1}H NMR spectra of **1c** (insert) and **2c**.

refined without restraints. The structures were refined by full-matrix least-squares on F^2 and calculations by either SHELX-TL 95[17] or SHELXL 97.[18] In the refinement of **4c**, the scale factor was allowed to vary by not setting a scale factor restraint. Absorption corrections were either fitted empirically by spherical harmonic functions[19] or with the SORTAV[20] programme.

CCDC reference number 186/1731.

See http://www.rsc.org/suppdata/dt/a9/a906949f/ for crystallographic files in .cif format.

Results and discussion

Synthesis of complexes

The condensation of 4-aminothiophenol and different *para*-substituted benzaldehydes resulted in formation of thiol imines (L) (Scheme 1), capable of functioning as monodentate ligands *via* the sulfur atom.

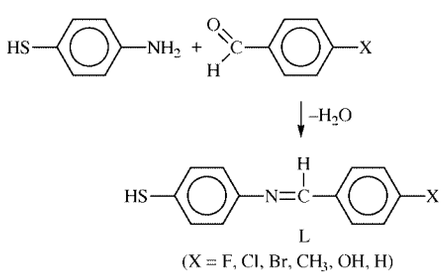

Scheme 1

These thiol imines had characteristic ν_{CN} stretching frequencies in their infrared spectra. The nature of X, where X is a halide, affects the stretching frequency the most when the halide is fluorine. The more electronegative fluorine is expected to decrease the N=CH double bond electron density, which should result in a lower ν_{CN} frequency. Hence it is not clear why the observed ν_{CN} for the fluoro compound is the highest. The chemical shifts observed in the ^{1}H NMR spectra appear to be invariant for the compounds **1a**–**6a** and show no effect of the substituents on the ligands. However, variation of X has some electronic influence on the electron density as shown by the electrochemical data (Table 2), discussed later.

The reactions of L with Ni(η^5-C_5H_5)(PR_3)Br (R = Ph, Bu), when the ligand was deprotonated by Et_3N, at room temperature produced the thiolato complexes, Ni(η^5-C_5H_5)(PR_3)(SC_6H_4N=CHC_6H_4X-4′) (Scheme 2). All the nickel complexes isolated, **1a**–**6b**, were dark-brown to dark green crystalline solids. Spectroscopic characterization, elemental analyses, mass spectrometry and subsequent single crystal X-ray diffraction

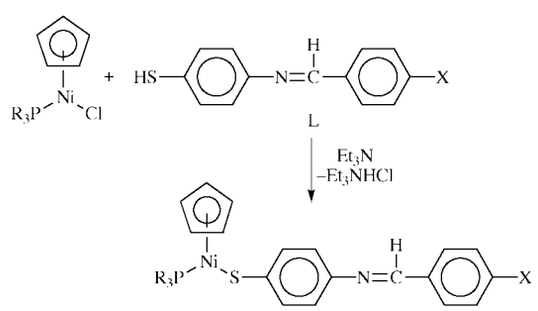

Scheme 2

studies of Ni(η^5-C_5H_5)(PPh_3)(SC_6H_4N=CHC_6H_4Br-4′) confirmed the products as formulated in Scheme 2.

The ^{1}H NMR spectra of complexes where X is a halide showed no significant chemical shift for the N=CH proton in the free ligand and when complexed. A similar observation was made by Silver *et al.* for the iminyl protons of Fe(η^5-C_5H_5)-(η^5-C_5H_4CH=NC_6H_4Y-4′) and *p*-$Me_2NC_6H_4$CH=NC_6H_4Y-4′ (Y = F, Cl, Br[21]), where the iminyl protons have chemical shifts ranging from 8.38–8.43 ppm. This peak was also indifferent to the phosphine used. The observed peak values for both phosphine ligands were 8.43 ppm (PPh_3) and 8.44 ppm (PBu_3). The major differences in the ^{1}H NMR spectra were found for the C_5H_5 ring chemical shifts. All the PPh_3 compounds had essentially the same chemical shift of 5.14 ppm, whilst the PBu_3 compounds had chemical shifts of 5.27 ppm. We reported a similar trend for 4-chlorothiophenolate complexes, Ni(η^5-C_5H_5)(PR_3)(SC_6H_4Cl-4′), with the same set of phosphines.[7c] This suggests that back-bonding from the Ni to PBu_3 is more extensive than to PPh_3. The back-bonding reduces the electron density on the nickel, which in turn draws electron density from the C_5H_5 ring and thus de-shields its protons. Further evidence of this is provided by the ^{31}P NMR spectra, where the PBu_3 peaks are more upfield than those of PPh_3 despite the former being a better σ-donor. The chemical shift values of *ca.* 35.4 ppm and *ca.* 22.4 ppm for all the PPh_3 and PBu_3 complexes respectively point to the lack of any effect of the *para*-substituents of the thiolate ligand on the ^{31}P NMR chemical shifts.

Each of the two phenyl groups in the thiolato ligands of the complexes exhibit a classical AA′BB′ spin system[22] in the ^{1}H NMR spectra and the spectrum of **2c** depicts this clearly (Fig. 1). The ^{1}H NMR spectral assignments for the C_6-ring were made by reference to the *para*-fluoro derivative. This is facilitated by the hydrogen–fluorine coupling, affording an easy way to assign the ring protons based on the labeling in structure **C**. Protons H_d and $H_{d'}$ appear as a doublet of doublets, as a result

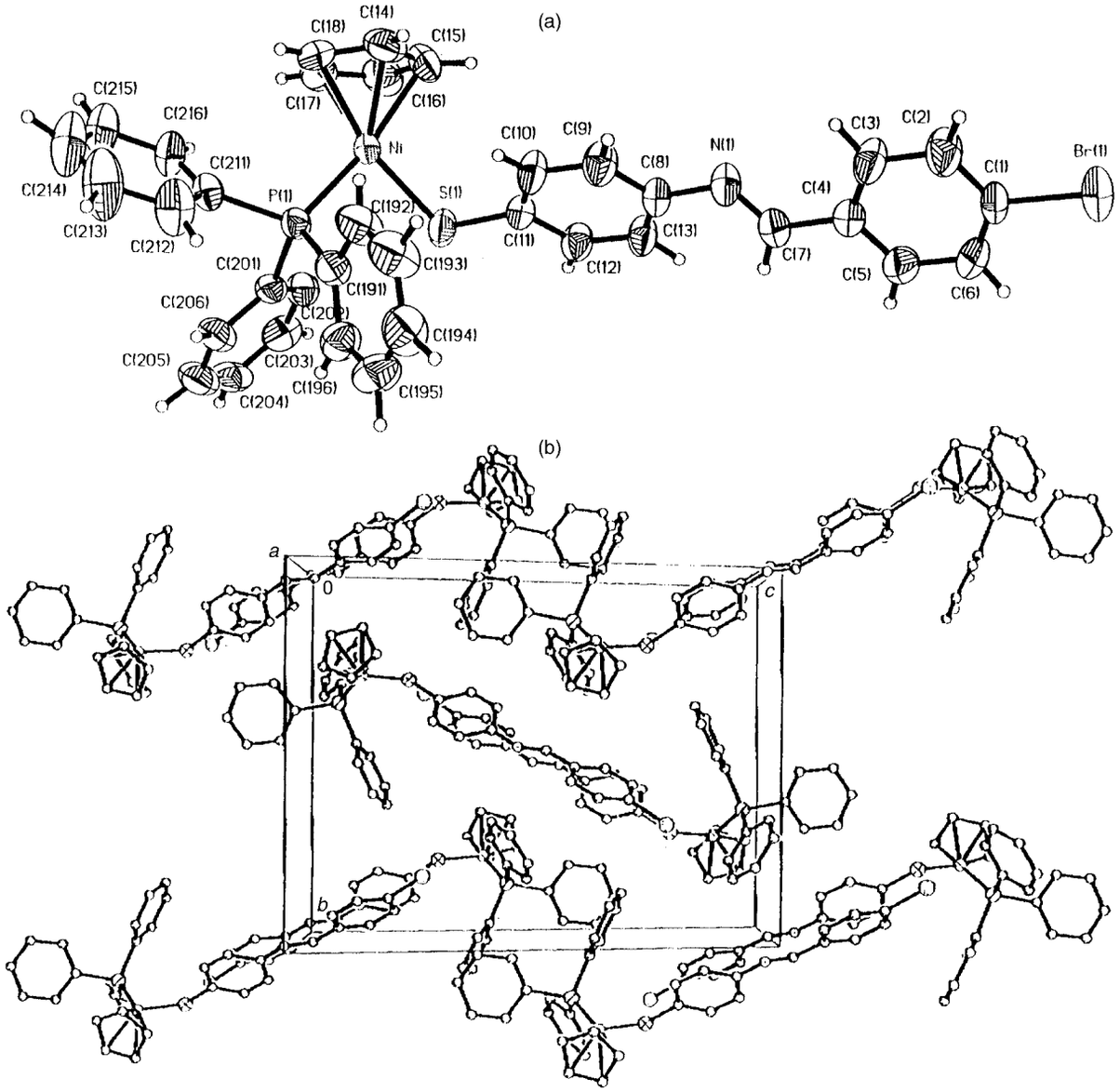

Fig. 2 (a) Crystal structure of **3b**. Selected bond distances (Å) and angles (°) are: Ni–S(1) 2.1834(10), Ni–P 2.1447(10), Cp–Ni 1.743, C(11)–S(1) 1.766(4), C(7)–N(1) 1.261(5), C(1)–Br(1); P(1)–Ni–S(1) 91.18(4), Ni–S(1)–C(11) 112.04(13). (b) Packing diagram of **3b**.

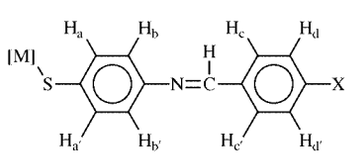

[M] = Ni(η^5-C_5H_5)(PBu_3)

C

of coupling of these protons with H_c and $H_{c'}$ and with the fluorine. Similarly, H_c and $H_{c'}$ are observed as a pseudo triplet from the same set of coupling. Thus for all complexes the most downfield doublets, doublet of doublets for the fluoro derivatives, are peaks of the H_d and $H_{d'}$ protons whilst H_c and $H_{c'}$ are the second most downfield peaks. By a similar argument the upfield doublets belong to H_a and $H_{a'}$.

When the mass spectra of compounds **1b**–**5b** were run using the soft FAB ionisation technique, all the compounds except **3b** showed molecular ions. However, even with the soft FAB ionization technique there was considerable fragmentation. All the compounds had fragments of *m/z* values of 385 and 647 as the dominant peaks in the spectra. These were identified as $[(\eta^5\text{-}C_5H_5)Ni(PPh_3)]^+$ and $[(\eta^5\text{-}C_5H_5)Ni(PPh_3)_2]^+$ respectively. The latter ion is a product of a re-arrangement in the mass spectrometer. From thermal gravimetric analysis (TGA) (*vide infra*), it could be established that **3b** readily decomposed at 180 °C whereas the rest of the complexes decompose above this temperature. It is therefore likely that the inability of **3b** to give a molecular ion, even in the FAB mode, could be due to thermal decomposition.

Molecular structures of 3b and 4c

The proposed structures from the analytical data were confirmed by single crystal X-ray diffraction studies of **3b** and **4c**. The structures are depicted in Fig. 2 and 3, with selected bond distances and angles. Of particular note in the structure of **4c** is a high residual electron density, about 0.3 Å from the nickel. This high residual electron density normally arises from inadequate treatment of data for absorption. But considering the absorption treatment applied to **4c**, the high residual electron density may be due to the quality of the crystal. The structures are typical of the structural motifs found for Ni(η^5-C_5H_5)(PR_3)(EC_6H_4Cl-4) (R = Ph, Bu; E = S, Se; X = H, Cl).[7a–c] They include similarities in Cp–Ni, Ni–P and Ni–S bond distances. Comparison of the C=N distances of the Schiff base ligands in **3b** and **4c** with the free thio Schiff base ligand, *N*,*N*′-bis(4-chlorobenzylidene)-2,2′-diaminodiphenyldisulfide[23] simi-

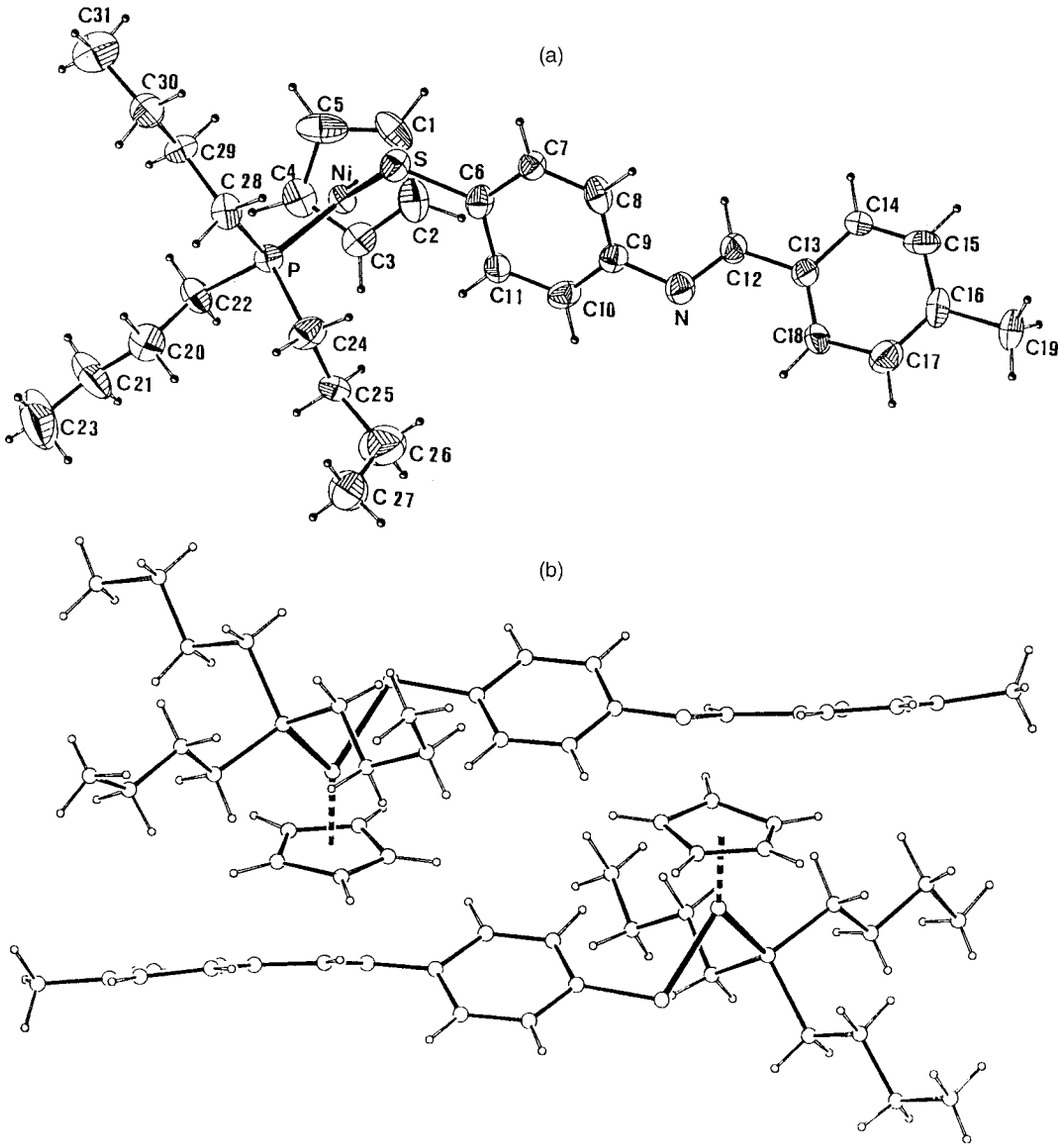

Fig. 3 (a) Crystal structure of **4c**. Selected bond distances (Å) and angles (°) are: Ni–S(1) 2.1483(12), Ni–P 2.1351(10), Cp–Ni 1.764, C(6)–S 1.752(5), C(12)–N 1.262(7), C(16)–C(19); P–Ni–S 92.32(5), Cp–Ni–P 132.8, Cp–Ni–S 134.8, Ni–S–C(6) 110.48(17). (b) Packing diagram of **4c**.

larly reveals no significant effect of the bonding interactions with the nickel. The C=N bond distances in the free disulfide ligand are 1.261(5) and 1.258(5) Å respectively,[23] whilst the C=N distances in **3b** and **4c** are 1.261(5) and 1.262(7) Å respectively. The most striking features of the structures are found in the molecular packing [Fig. 2(b) and 3(b)]. Both have pair-wise association of molecules in a donor (D)–π-acceptor (A) DAAD type packing, with the cyclopentadienylnickel phosphino end of the molecule as donor and the Schiff base ligand as the acceptor. This DAAD type of packing is best depicted by **3b** when the packing is viewed along the *a*-axis [Fig. 2(b)]. From this view the C_6-ring arrangement of the thio ligand from each molecule are 4.5–5.2 Å apart.[24] In both molecules the two C_6-rings are in different planes, at right angles to each other. Another interesting feature of the packing is the orientation of the cyclopentadienyl rings. Again, in both molecules the cyclopentadienyl rings are oriented in different directions away from the pair-wise array of the rings. This allows the thio ligands to pack in an almost DAAD fashion in **3b**, but in **4c** the ring with the methyl substitution is bent away from the rest of the molecule to avoid steric crowding. The DAAD structural motif is similar to that observed in the ferrocenyl Schiff base compounds $Fe(\eta^5\text{-}C_5H_5)(\eta^5\text{-}C_5H_4CH{=}NC_6H_4NO_2\text{-}4')$.[21] This type of stacking normally gives rise to C_6-ring π–π interactions, which exists in the ferrocenyl compound above with ring distances of 3.478 Å. However, the inter-ring distances in **3b** imply there is no such π–π interaction.

Table 2 Electrochemical data for PPh_3 and PBu_3 complexes

Complex	Reduction potential/V	Oxidation potential/V	Δ*E*/V
1b	0.197	0.509	0.312
2b	0.208	0.460	0.252
3b	—	0.439	—
4b	0.202	0.456	0.254
5b	0.210	0.476	0.266
1c	0.299	0.420	0.121
2c	0.312	0.418	0.106
3c	0.324	0.405	0.081
4c	0.301	0.394	0.093

Electrochemical studies

Cyclic voltammograms of **1b**–**5b** and **1c**–**4c** were measured in CH_2Cl_2, with two representative voltammograms shown in Fig. 4. The results of the electrochemistry of the complexes are summarized in Table 2. Complexes **1b**–**5b** showed irreversible redox behaviour, whereas **1c**–**4c** were quasi-reversible. The triphenylphosphine complexes had ill-defined reduction

Table 3 Thermal analysis of selected complexes

Compounds	Weight loss[a] (%)	Temperature range[b]/°C	Peak value[b]/°C	ΔH^b/ kJ mol^{-1}
3b	4.80, 20.78	138.1–151.9	145.2	2.67
1c	41.18 (43.58)	102.2–114.9	109.6	46.22
2c	11.78 (11.95)	82.0–94.1	89.4	41.04
3c	19.31, 16.71	78.5–93.6	88.4	28.16
4c	43.49 (43.15)	77.4–90.1	84.5	41.92

[a] Data from TGA (calculated weight loss in brackets). [b] Data from DSC.

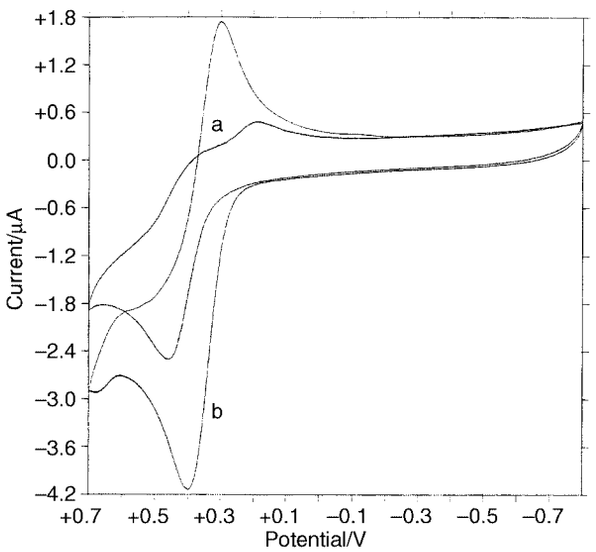

Fig. 4 Cyclic voltammograms of (a) **4b** and (b) **4c**.

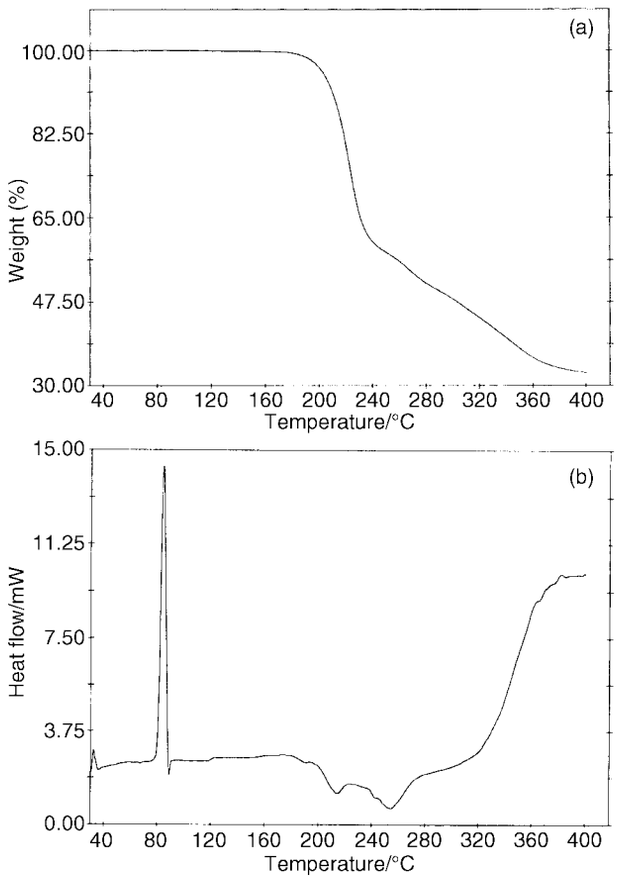

Fig. 5 Thermal analysis of **4c**: (a) TGA and (b) DSC.

peaks, whereas the tributylphosphine compounds exhibited well-defined reduction and oxidation peaks. The effect of the phosphine ligands on the electrochemical behaviour of the compounds was evident when triphenylphosphine was replaced with tributylphosphine (Fig. 4). Apart from **1c**–**4c** being easier to oxidize, the quasi-reversibility of these compounds could be attributed to stabilization of the electroactive species by the more basic PBu_3 as compared to PPh_3. The voltammograms also indicate that a faster transfer kinetics is operational in complexes with the tributylphosphine ligand. The trend in the peak potentials of the halide derivatives (Table 2) was similar regardless of the phosphine. It appears the more electronegative halide derivatives were more difficult to oxidize, but it is difficult to see how these substituents could influence the ease of electron removal from the nickel centre. This trend, though, and the rest of the redox properties are similar to that found for Ni(η^5-C_5H_5)(PR_3)(SC_6H_4X-4′) (R = Ph, Bu; X = Cl, Br).[7c]

Thermal properties of 1c–4c and 3b

The thermal properties of selected complexes were investigated by thermogravimetric analysis (TGA) and by differential scanning calorimetry (DSC). Their thermal behaviour is typified by **4c** (Fig. 5). Table 3 shows the rest of the thermal analysis data. All the complexes decomposed above 180 °C, except **3b,** which decomposed at 180 °C. In the TGA, decomposition was generally *via* the loss of the thioimine ligand (L), except for **2c** and **3b**. The chloro derivative, **2c**, showed loss of the cyclopentadienyl ligand; whereas **3b** showed two successive losses of 4.80% and 20.78% that could not be attributed to any logical fragmentation sequence. The DSC data was obtained by two heating and cooling cycles to confirm the authenticity of the data. All complexes investigated gave endothermic peaks with ΔH values ranging from a low of 2.67 kJ mol^{-1} for **3b** to a high of 46.22 kJ mol^{-1} for **1c** (Table 3). The onset of the endothermic peaks in these complexes depends on two factors. First the PPh_3 complex **3b** had a higher onset temperature, accompanied by a low ΔH (Table 3). For the PBu_3 complexes (**1c**–**4c**) the onset of the endothermic peak was at much lower temperatures and decreased with the electronegativity of the *para*-substituent. The lowest temperature was observed for the CH_3 analogue (**4c**). This appears to indicate that the nickel end of the molecule needs electron density on the metal, whereas the other end is less electron rich. The high values of the endothermic peaks could be due to heat associated with mesophase changes.[25] We are currently performing experiments to establish whether these complexes are indeed liquid crystalline.

Conclusions

Schiff base nickel complexes that have the ligands bound to the metal *via* a sulfur atom are readily prepared. The PBu_3 complexes show the onset of endothermic peaks in their DSC at temperatures ranging from 77.4 to 102.2 °C. Lower onset temperatures are associated with complexes containing less electron withdrawing groups in the 4′-position of the Schiff base ligand. The effect of the substituent can also be seen in the case of oxidation of the nickel centre as established from cyclic voltammetric studies. In this regard, the compounds with electron withdrawing substituents are more difficult to oxidise.

Acknowledgements

Financial support from the National Research Foundation (NRF), South Africa, is gratefully acknowledged. One of us (F. A. N.) thanks the NRF and ESKOM, South Africa for bursary support. We are grateful to Ms. Leanne Cook, University of the Witwatersrand, South Africa and Dr John Bacsa, University of Cape Town, South Africa, who determined the structures as a service. Finally we wish to thank Ms.

Ayesha Jacobs, University of Cape Town for the thermal analysis and Mr Tim Lesch, University of the Western Cape, for the elemental analysis.

References

1 (*a*) Y. Sugiura and Y. Hirayama, *Inorg. Chem.*, 1976, **15**, 679; (*b*) L. Casella, *Inorg. Chem.*, 1984, **23**, 679.
2 Y. Elerman and I. Svoboda, *Acta Crystallogr.*, *Sect. C*, 1996, **52**, 2705.
3 (*a*) R. G. Charles and H. Freiser, *J. Org. Chem.*, 1953, **18**, 422; (*b*) H. Jadamus, Q. Fernando and H. Freiser, *J. Am. Chem. Soc.*, 1964, **86**, 3056; (*c*) Y. Sugiura, Y. Hirayama, T. Tanaka and K. Ishizu, *J. Am. Chem. Soc.*, 1975, **97**, 5577; (*d*) S. Ide, S. G. Öztas, N. Ancin and M. Tüzün, *Cryst. Res. Technol.*, 1996, **31**, 427.
4 L. F. Lindoy and S. E. Livingstone, *Inorg. Chem.*, 1968, **7**, 1149.
5 D. E. Wheeler, S. T. Hill, S. Milos, J. D. Williams and J. D. Johnson, *J. Organomet. Chem.*, 1997, **530**, 83 and references therein.
6 W. E. Lindsell and L. Xinxin, *J. Chem. Res.* (*S*), 1998, 62 and references therein.
7 (*a*) J. Darkwa, F. Bothata and L. M. Koczon, *J. Organomet. Chem.*, 1993, **455**, 235; (*b*) J. Darkwa and W. Milius, *Acta Crystallogr.*, *Sect. C*, 1996, **52**, 2159; (*c*) J. Darkwa, R. M. Moutloali and T. Nyokong, *J. Organomet. Chem.*, 1998, **564**, 37.
8 (*a*) P. Espinet, M. A. Esteruelas, L. A. Oro, J. L. Serrano and E. Sola, *Coord. Chem. Rev.*, 1992, **117**, 215; (*b*) S. A. Hudson and P. M. Maitlis, *Chem. Rev.*, 1993, **93**, 861; (*c*) M. Ghedini, D. Pucci, A. Crispini and G. Baberio, *Organometallics*, 1999, **18**, 2116; (*d*) M. Lee, Y.-S. Yoo and M.-G. Choi, *Macromolecules*, 1999, **32**, 2777.
9 R. Pache, H. Zaschke, A. Madicke. J. R. Chipperfield, A. B. Blake, P. G. Nelson and G. W. Gray, *Mol. Liq. Cryst. Lett.*, 1988, **6**, 81.
10 J. Malthête and J. Billard, *Mol. Liq. Cryst. Lett.*, 1976, **34**, 117.
11 K. Ohta, H. Ema, I. Yamamoto and K. Matsuzaki, *Liq. Cryst.*, 1988, **3**, 1671.
12 K. Ohta, H. Ema, Y. Morizumi, T. Watanabe, T. Fujimoto and I. Yamamoto, *Liq. Cryst.*, 1990, **3**, 311.
13 (*a*) A.-M. Giroud and U. T. Müller-Westerhoff, *Mol. Cryst. Liq. Cryst.*, 1977, **41**, 11; (*b*) A.-M. Giroud, *Ann. Phys.* (*Paris*), 1978, **3**, 47; (*c*) A.-M. Giroud, A. Nazzal and U. T. Müller-Westerhoff, *Mol. Cryst. Liq. Cryst.*, 1980, **56**, 225; (*d*) U. T. Müller-Westerhoff, A. Nazzal, R. J. Cox and A.-M. Giroud, *Mol. Cryst. Liq. Cryst.*, 1980, **56**, 249; (*e*) M. Cortrait, J. Gaultier, C. Polycarpe, A.-M. Giroud and U. T. Müller-Westerhoff, *Acta Crystallogr.*, *Sect. C*, 1983, **39**, 833.
14 K. W. Barnett, *J. Chem. Educ.*, 1974, **51**, 422.
15 J. Darkwa, *Organometallics*, 1994, **13**, 4734.
16 M. S. Thomas, J. Darkwa, E. Y. Osei-Twum and L. A. Latorja, Jr., *Polyhedron*, 1999, **18**, 2803.
17 G. M. Sheldrick, SHELXTL 95, Program for the Refinement of Crystal Structures, University of Göttingen, Germany, 1995.
18 G. M. Sheldrick, SHELXTL 97, Program for the Refinement of Crystal Structures, University of Göttingen, Germany, 1997.
19 G. M. Sheldrick, SADABS, An Empirical Absorption Correction, private communication to subscribers of the Siemens CCD e-mail list.
20 R. H. Blessing, *J. Appl. Crystallogr.*, 1997, **30**, 421.
21 A. Houlton, N. Jasim, R. M. G. Roberts, J. Silver, D. Cunningham, P. McArdle and T. Higgins, *J. Chem. Soc.*, *Dalton Trans.*, 1992, 2235.
22 H. Freibolin, *Basic one- and two-dimensional NMR spectroscopy*, VCH, New York, 2nd edn., 1993, p. 121.
23 S. Ide, S. G. Öztas, N. Ancin and M. Tüzün, *Acta Crystallogr.*, *Sect. C*, 1997, **53**, 376.
24 Inter-ring distances were determined with the program PLATON; A. L. Spek, University of Utrecht, The Netherlands, 1995.
25 M. E. Brown, *Introduction to Thermal Analysis*, *Techniques and Applications*, Chapman and Hall, London, 1988, p. 43.

Paper a906949f